

Evaporating crystallization effect of ammonium sulfate at atmospheric pressure under the action of ultrasound

Haoran Xu^{a,b}, Guang Fu^c, Duclenh Phan^d, Liuxin Xiang^{a,b}, Thiquynhuan Le^{a,b,*}, Libo Zhang^{a,b,*}

^a State Key Laboratory of Complex Non-ferrous Metal Resources Clean Utilization, Kunming University of Science and Technology, Kunming 650093, Yunnan, China

^b Faculty of Metallurgical and Energy Engineering, Kunming University of Science and Technology, Kunming 650093, Yunnan, China

^c Yunnan Chihong Zinc and Germanium Co., Ltd., Qujing 655011, Yunnan, China

^d Science and Technology Center, MienTrung Industry and Trade College, Phu Yen province 56000, VietNam

ARTICLE INFO

Keywords:
Ultrasound
Crystallization
Ammonium sulfate
Atmospheric evaporation

ABSTRACT

Ultrasound enhanced evaporating crystallization has been proposed to solve the problems of low crystallization yield and uneven particle size in the evaporating crystallization process of ammonium sulfate solution at atmospheric pressure. The effects of key operating parameters, including the ultrasound power, stirring speed, pH value, and ultrasound time, on the yield of ammonium sulfate product and the duration of solid-liquid transformation time are studied. The results show that the ultrasound crystallization can increase the ammonium sulfate yield by 52.9 %, reduce the solid-liquid transformation time of ammonium sulfate by 10 %, and obtain ammonium sulfate products with higher crystallinity and more uniform particle size. Ultrasound promotes the crystallization of ammonium sulfate by enhancing the transfer of heat in the solution and reducing the super-solubility of the ammonium sulfate solution from 937.5 g/L to 833.33 g/L. This study provides experimental justification for the use of ultrasound in atmospheric evaporative crystallization.

1. Introduction

Ammonium sulfate has garnered attention for its application in agricultural chemical fertilizer, rare earth leaching, battery production and recycling processes[1–6]. Using flue gas with a low concentration of sulfur dioxide produced by metal smelting to produce ammonium sulfate fertilizer has important environmental protection and sulfur resource utilization significance. The principle of ammonia desulfurization is to convert sulfur dioxide in flue gas into an ammonium sulfate solution through ammonia absorption and oxidation, and subsequently obtain ammonium sulfate products from the ammonium sulfate solution through crystallization. The crystallization step plays a key role in determining product quality and production costs.

At present, the methods used to crystallize ammonium sulfate include the addition of seed crystals, vacuum crystallization, antisolvent crystallization, and atmospheric pressure crystallization. By adding large particles of ammonium sulfate, other metal salts, fly ash, and urea [7,8], ammonium sulfate grows on these large particles, which plays a role in inhibiting the spontaneous formation of small grains[9–12].

Although the addition of seed crystals can produce ammonium sulfate products with uniform particles and large particle sizes, there are strict requirements on the addition time and amount and the process operation is cumbersome[13]. Ammonium sulfate products with larger particles and regular shapes can be obtained at lower temperatures and without crystal seeds when using vacuum crystallization. However, the use of vacuum crystallization needs to ensure the sealing performance of the evaporator and requires additional expenditure. Antisolvent crystallization involves the precipitation of solute in solution by the addition of an organic solvent that is miscible with the aqueous solution[14], but there are problems such as high cost and separation of the organic solvent after the reaction. Atmospheric evaporating crystallization is heated by steam and flue gas waste heat without the need for a vacuum device, which has the advantages of a simple process and low processing cost. However, the evaporating crystallization at atmospheric pressure results in a low ammonium sulfate crystallization yield, poor crystal quality, uneven particle size distribution, and irregular morphology, which not only cause economic losses, but also tend to agglomerate when fertilized due to poor crystallization, which limits its application.

* Corresponding authors.

E-mail addresses: quynhluanlt@kust.edu.cn (T. Le), zhanglibopaper@126.com (L. Zhang).

<https://doi.org/10.1016/j.ultsonch.2024.106896>

Received 25 February 2024; Received in revised form 11 April 2024; Accepted 3 May 2024

Available online 4 May 2024

1350-4177/© 2024 The Author(s). Published by Elsevier B.V. This is an open access article under the CC BY-NC-ND license (<http://creativecommons.org/licenses/by-nc-nd/4.0/>).

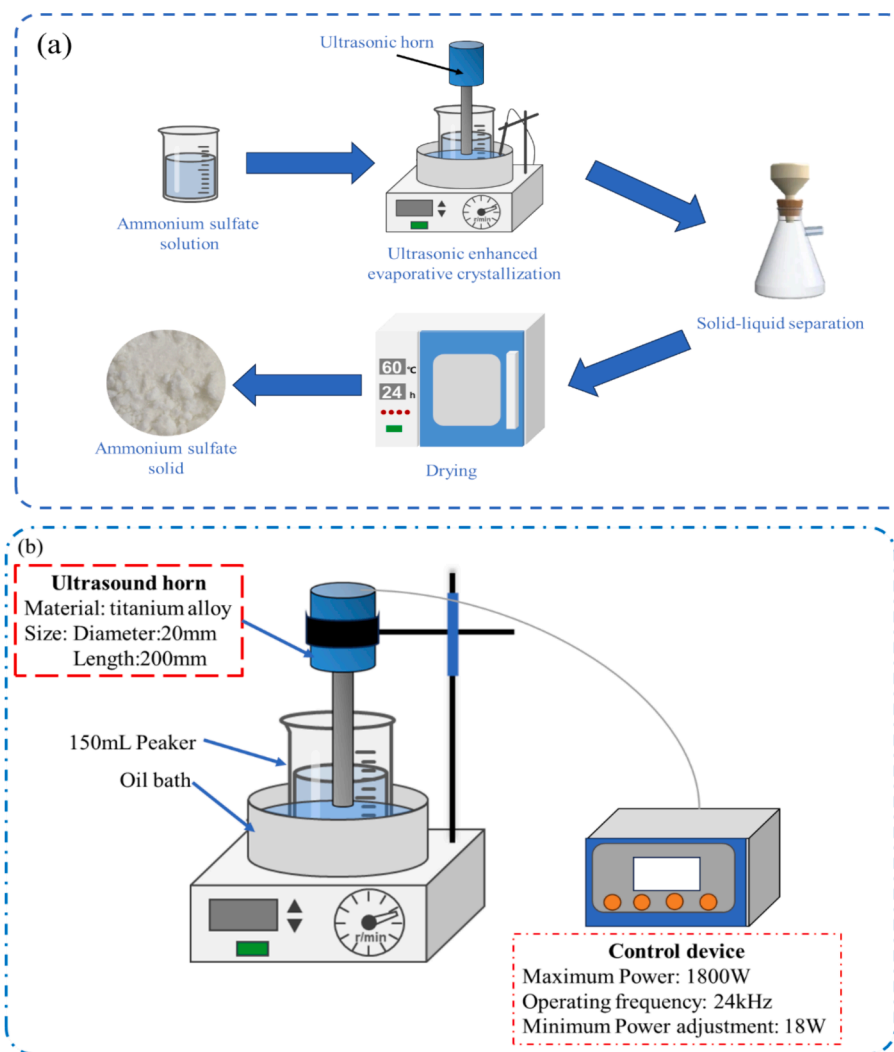


Fig. 1. The experimental flowchart(a) and schematic diagram of the ultrasound device(b).

[15].

As a mechanical wave with a frequency greater than 20 kHz, ultrasound can form high-temperature and high-pressure cavitation bubbles in water. When these cavitation bubbles rupture, high-speed microjets and shock waves are generated locally, causing changes in the solid-liquid interface energy, resulting in fine grains in the solution. Ultrasound crystallization process is widely used in the crystallization production of food and medicine due to the advantages of not needing to add seeds and having an adjustable crystal size. Ghosh et al. [16] used ultrasound evaporating crystallization to produce 2,4,6,8,10,12-Hexanitro-2,4,6,8,10,12-hexaazaisowurtzitane (CL-20) and found that after ultrasound evaporating crystallization, CL-20 had a high true density with a decreased percentage of voids, decreased total moisture content and no agglomeration. Hu et al. [17] used ultrasound evaporation to crystallize sucrose solution. The results indicated that not only was the viscosity of sugar solution reduced, but also that the heat transfer coefficient and evaporation intensity of the evaporation system improved by 42.4 % and 15.2 %, respectively, and that the scale was removed remarkably, with no significant effects on white sugar quality. The above research showed that ultrasound has a strengthening effect on evaporating crystallization. Ultrasound has been reported to promote ammonium sulfate crystallization, but existing research has focused mainly on ultrasound enhanced cooling crystallization [18] and ultrasound-induced nucleation of saturated solution as seeds for cooling crystallization [19]. There are few reports on the effect and mechanism

of ultrasound waves on the evaporating crystallization of ammonium sulfate.

In this work, an unsaturated simulated ammonium sulfate solution with similar concentration to the actual production of ammonium sulfate was used for the evaporation crystallization experiment. The solid-liquid transformation time (t_{trans}) was defined as the time when an ammonium sulfate solution was heated from room temperature to precipitated crystal in this work. The strengthening effect of ultrasound was analyzed by comparing the quality of the quality of recovered crystals and the transformation time. The product morphology, crystallization effect and crystal particle size of ammonium sulfate samples were compared under different conditions of ultrasound-assisted evaporating crystallization process, and the mechanism underlying the influence of ultrasound was explored.

2. Experimental

2.1. Materials and analytical methods

The simulated desulfurization solution was prepared according to the actual solution composition during production, specifically containing a sulfate content of 300 g/L and a sulfite content of 20 g/L. The ammonium sulfite and ammonium sulfate used in this experiment were produced by Shanghai Aladdin Biochemical Technology Co., Ltd. The ultrasound generator (maximum ultrasound intensity: 1800 W,

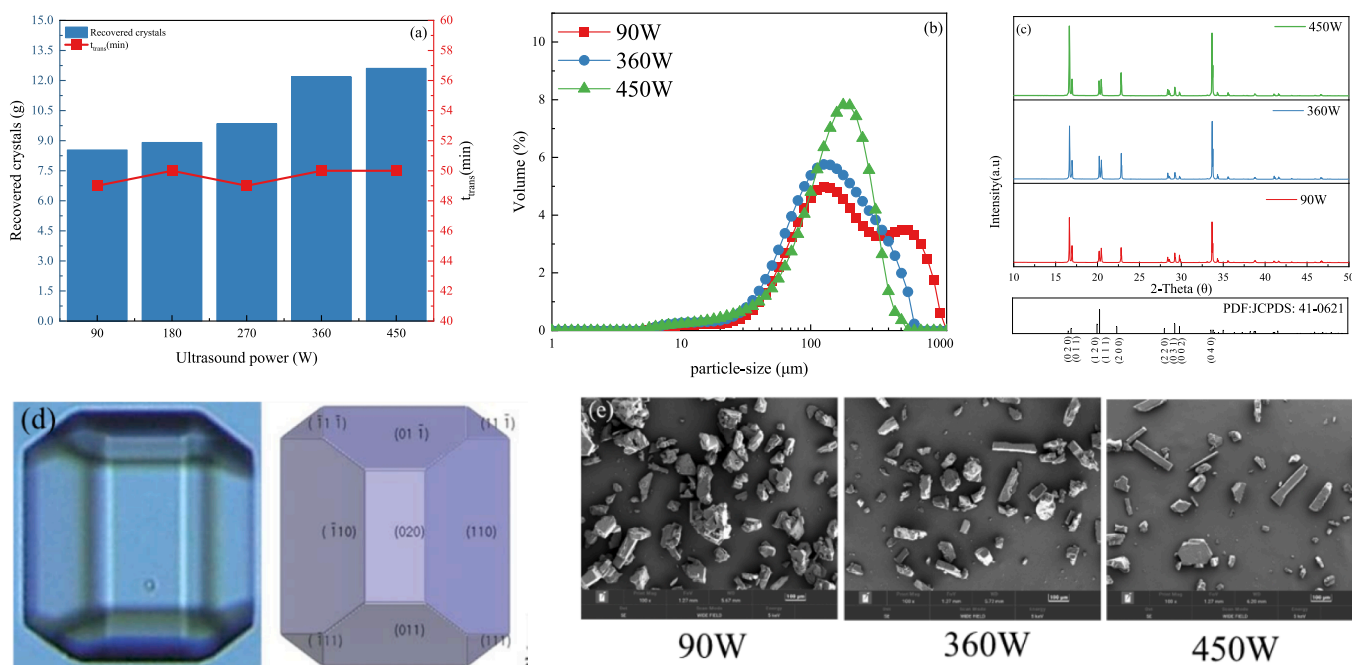


Fig. 2. Effect of ultrasound power on the quality of recovered crystals and transformation time(a), on crystal particle size(b), crystal plane (c) and micromorphology (e) of the ammonium sulfate. The orthorhombic structure with nomenclature of specific faces of ammonium sulfate(d) [22].

operating frequency: 24 kHz) used in this experiment was produced by Shanghai Weimi Technology Co., Ltd. The ultrasound generator consisted of an ultrasound horn and a control device, which could achieve a minimum of 1 % (18 W) ultrasound power adjustment. The ultrasound horn was made of titanium alloy. The size of the horn was 20 mm in diameter, and a 200 mm in length immersion of the tip directly into the solution provided a direct mode of irradiation. An X-ray diffractometer (Rigaku dX 2000, Cu-Ka radiation, operating at 40 kV and 25 mA) was used to analyze the crystal planes of ammonium sulfate after crystallization. The morphology of the crystals were analyzed by scanning electron microscopy (Philips XL20 ESEM-TMP, Amsterdam, The Netherlands). The particle size distribution of the products was determined by a laser particle size analyzer (Mastersizer 2000, UK).

2.2. Experimental procedure

Evaporating crystallization is heated by the steam waste heat of industrial steam with temperatures of 120–140 °C [20,21]; therefore, the temperature of the oil bath pot, which is the heat source, is fixed at 135 °C in our experiment. In each experiment, 75 mL of ammonium sulfate solution was transferred to a 150 mL beaker, and an ultrasonic horn was inserted to ensure that the bottom of the horn was 35 mm below the liquid surface. The solution was heated from room temperature (about 25 °C) using an oil bath, and the entire heating time was fixed at 60 min. During the reaction process, a magnetic stirrer with a length of 32 mm and a diameter of 5 mm was used to stir the solution, and an appropriate ultrasonic start time was selected according to the experimental requirements. When observable grains are produced in the solution, the timing is stopped, and the time is recorded as the solid–liquid transformation time (t_{trans}). The solution was further heated until the heating time reached 60 min, after which the produced ammonium sulfate was filtered. The beaker was rinsed with alcohol to obtain the remaining ammonium sulfate. After drying at 65 °C for 12 h, the ammonium sulfate product was taken for further analysis. The experimental flowchart and the schematic diagram of the ultrasound device are shown in Fig. 1(a) and (b), respectively.

3. Results and discussions

3.1. Effect of ultrasound on the evaporating crystallization of ammonium sulfate at atmospheric pressure

3.1.1. Effect of ultrasound power

The effects of ultrasound power on the transformation time (t_{trans}) and the quality of the quality of recovered crystals were studied at a stirring rate of 100 RPM, a solution pH of 7, and an ultrasound time of 60 min under different ultrasound powers (90, 360 and 450 W), and the results are shown in Fig. 2(a). The particle sizes, XRD patterns and SEM images of ammonium sulfate products under different ultrasound powers are shown in Fig. 2(b), (c), and (e), respectively. The crystal plane of the ammonium sulfate was identified using a standard XRD card (JCPDS: 41–0621). The standard crystal form of ammonium sulfate and the position of each crystal plane are shown in Fig. 2(d).

As shown in Fig. 2(a), an increase in ultrasound power has little impact on the transformation time (t_{trans}), which remains at 49–50 min, but has a significant impact on the ammonium sulfate yield. In the range of 90 to 360 W, the crystallization yield increases from 8.53 g to 12.18 g, and the yield increases by only 0.43 g when the ultrasound power increases from 360 to 450 W. As the ultrasound power increases, the distribution width of the product particle size becomes narrower, as shown in Fig. 2(b), indicating that the particles are more uniform, but the average particle size of products decreases. Specifically, the average particle size of ammonium sulfate decreases from 262.17 μm at 90 W to 175.73 μm at 360 W, and finally to 166.38 μm at 450 W. Fig. 2(c) shows that the characteristic peak intensity of ammonium sulfate becomes significantly stronger when the ultrasound power increases from 90 to 360 W, indicating that increasing the ultrasound power within this range promotes the crystallization of the product. It was also found that the peak intensity of each crystal face of the ammonium sulfate product increases evenly at this time. However, this trend changes when the ultrasound intensity increases from 360 W to 450 W. The peak heights of the (020) and (040) crystal planes of the product under 450 W are significantly higher than those under 360 W, but the other crystal plane peaks are basically the same as those under 360 W.

Fig. 2(e) shows that the morphology of ammonium sulfate at 90 W

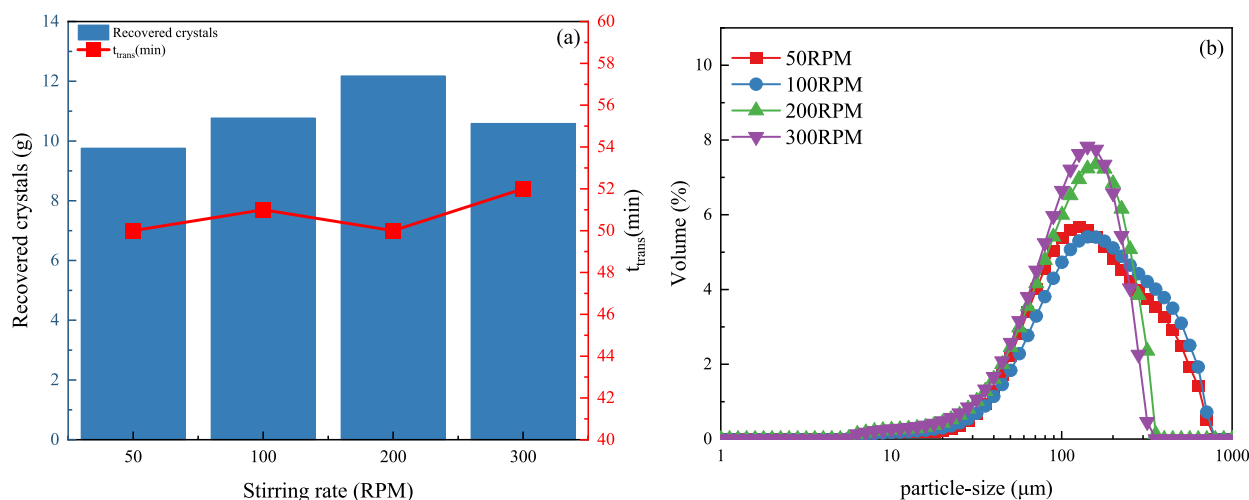


Fig. 3. Effect of stirring rate on the quality of recovered crystals and t_{trans} (a), and on crystal particle size (b).

included more large particles with uneven sizes obtained from the agglomeration of multiple orthorhombic particles. A stronger high-speed microjet is generated when the ultrasound power increases [23,24], which produces a significant shear impact on the particle surface, leading to the breakage of agglomerated large particles in the product and the formation of more uniform particles. As a result, large particles are dispersed to form more small particles with a morphology close to that of the standard orthorhombic crystal system at 360 W. The ammonium sulfate particles gradually transform from the orthorhombic crystal system to the slender flake particles when the ultrasound intensity increases from 360 W to 450 W (Fig. 2(e)) due to the overgrowth of the (040) and (020) crystal planes (Fig. 2(c)). The (020) and (040) crystal planes are the crystal planes perpendicular to the observation angle, as shown in Fig. 2(d). According to the existing research [25], the (020) plane and (040) plane in orthorhombic crystals cannot be matched with other crystal planes, so they are not suitable for the production of uniform orthorhombic ammonium sulfate particles. In addition, compared with orthorhombic crystal particles, slender flake particles are more easily broken, which is not conducive to the use of ammonium sulfate fertilizer. Therefore, the optimal experimental conditions for subsequent experiments are determined to be 360 W. The regulatory effect of ultrasound power on particle morphology has also been reported in other studies. Yang et al. [26] studied the effect of ultrasound on the crystallization of selenium and reported that as the

ultrasound power increased, the selenium crystals split from large particles into more small selenium particles with a columnar structure and gradually grew into selenium nanorods. Lucija Majal et al. [27] also found that an increase in ultrasound power caused the transformation of the ticagrelor crystals from agglomerated cubes to agglomerated rods, and finally to agglomerated needles, indicating that an increase in ultrasound power could transform large particles into smaller particles with more uniform particle sizes.

3.1.2. Effect of stirring rate

The effects of stirring rate on t_{trans} and the quality of recovered crystals were investigated under the conditions of an ultrasound power of 360 W, ultrasound time of 60 min and solution pH of 7 with different stirring rates (50, 100, 200, 300 RPM), the results are shown in Fig. 3(a). The particle sizes of different products were determined, as shown in Fig. 3(b).

The effect of increasing the stirring rate on the ammonium sulfate yield exhibits an upward trend from 50 RPM to 200 RPM (Fig. 3(a)). This can be attributed to the increase in collision frequency resulting from the increase in stirring rate. Such collisions include those between crystals and between crystals with the stirrer, consequently leading to an increase in the nucleation rate [28]. However, an excessively fast stirring speed results in small crystals being pushed to the container wall above the solution, which reduces the amount of small crystals produced in the

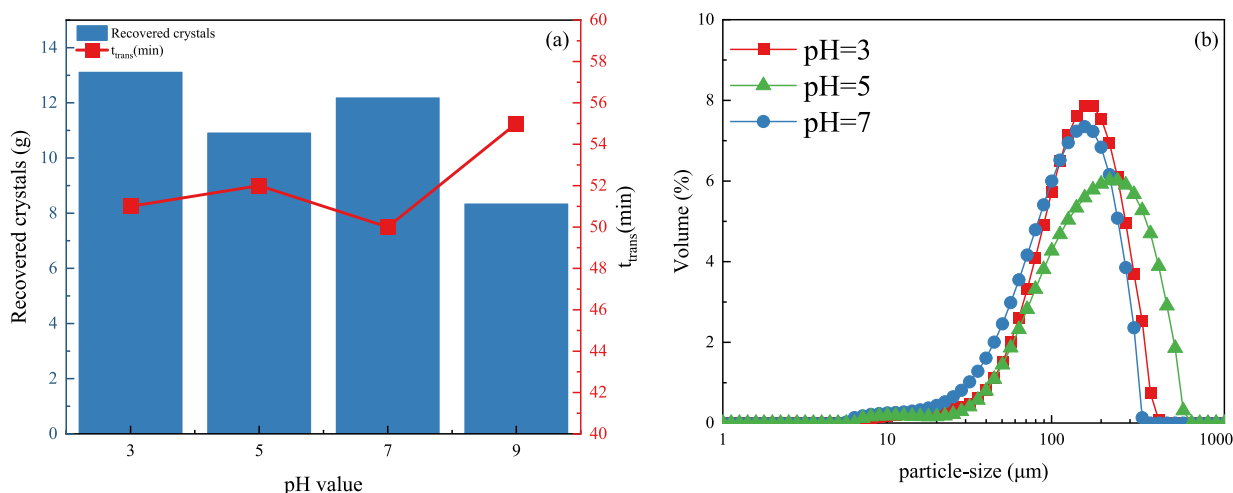


Fig. 4. Effect of pH value on the quality of recovered crystals and t_{trans} (a), and on crystal particle size (b).

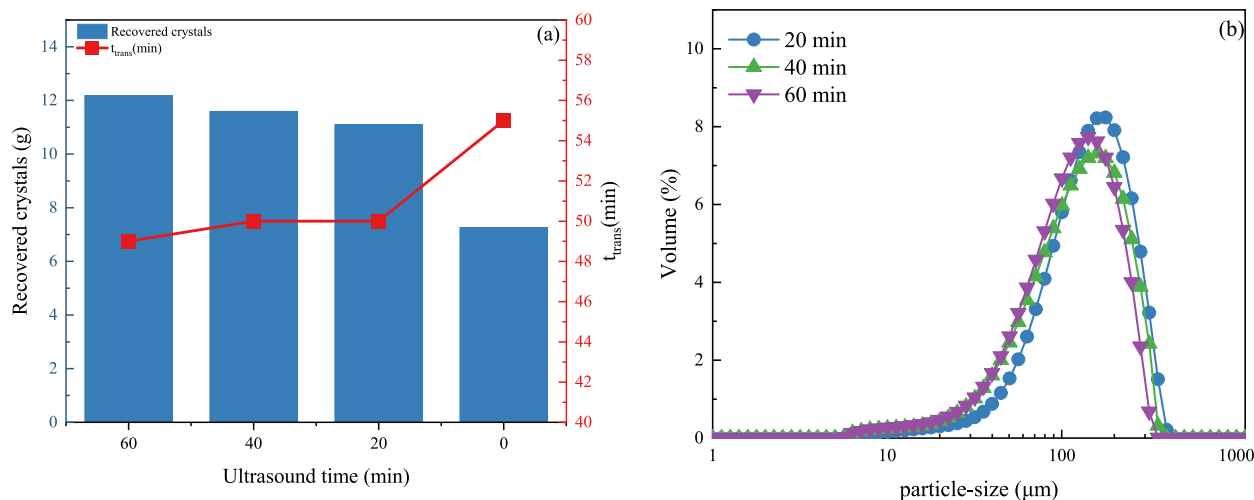


Fig. 5. Effect of ultrasound time on the quality of recovered crystals and t_{trans} (a), and on crystal particle size (b).

solution and ultimately hinders the crystallization process [18]. Therefore, an increase in the stirring speed from 200 to 300 RPM results in a decrease in ammonium sulfate yield. An increase in the stirring rate results in a more uniform mixing of the crystallization system, avoids the generation of large crystals due to excessive local supersaturation, accelerates the fragmentation of large crystal particles, and thereby obtains more uniform and smaller particles. As shown in Fig. 3(b), the particle size of the product decreases and their particle size distribution becomes narrower with the increase of stirring rate. Within the investigated stirring rate range, the change in t_{trans} remains within 50–52 min, indicating that an increase in the stirring rate can not significantly accelerate the precipitation of crystals. Therefore, 200 PRM is selected as the optimal condition.

3.1.3. Effect of pH value

The effects of the solution pH value on the t_{trans} and the quality of recovered crystals were studied at an ultrasound power of 360 W, an ultrasound time of 60 min, and a stirring rate of 200 RPM at different pH values (3, 5, 7 and 9), and the results are shown in Fig. 4(a). The pH value was adjusted through the addition of concentrated sulfuric acid (98 % AR grade) and ammonia (20 % AR grade). The particle sizes of different products were determined, as shown in Fig. 4(b).

The effect of pH value on the t_{trans} and the quality of recovered crystals does not show a direct correspondence due to the addition of concentrated sulfuric acid or ammonia, which can change the volume of the solution. The volume of desulfurization solution at pH = 9 is increased from 75 mL to 78.5 mL, therefore the t_{trans} is higher than that under other pH conditions, and the ammonium sulfate yield obtained under the same heating at pH of 9 is lower. In other words, a pH value of 9 is not conducive to the crystallization of ammonium sulfate.

Due to the strong acidity of concentrated sulfuric acid, the volume of the desulfurization solution does not change much when adjusted to acidic pH values. When the pH value drops from 7 to 5 or 3, the volume of the desulfurization solution increases from 75 mL to 75.4 or 75.8 mL. As the acidity of the desulfurization solution increases, the supersaturation required for ammonium sulfate crystallization decreases, and the ammonium sulfate crystal nuclei more easily precipitate. As a result, the desulfurization solution with pH = 3 has a higher ammonium sulfate yield and lower t_{trans} than the solution with pH = 5. Research by Mohod et al. [18] also showed that, compared with those under other pH conditions, the size of ammonium sulfate particles obtained at pH values of 5–5.5 was larger, and the nucleation and growth time of larger ammonium sulfate particles were longer. The average particle size of ammonium sulfate product at pH = 5 was confirmed to be larger than the average particle size of the product at pH = 3 as shown in Fig. 4(b) in our

work. The pH value of the desulfurization simulation solution was 7. The volume of the solution at pH = 7 is smaller than that at other pH values due to no need to add additional sulfuric acid or ammonia, therefore, the t_{trans} at pH = 7 is less than other pH values. Compared with that at pH = 3, the particle size distribution of ammonium sulfate at pH = 7 is narrower and the particles are more uniform, but the yield is slightly lower. However, the free acid content in ammonium sulfate fertilizer needs to be controlled according to Chinese national standards, and the free acid content exceeds the standard when evaporating crystallization at pH = 3. The pH of the ammonium sulfate solution during evaporating crystallization in actual production is 7–8, thus pH = 7 is selected as the optimal condition in this study.

3.1.4. Effect of ultrasound time

The total crystallization time was controlled to 60 min. The four conditions of normal heating 60 min (recorded as ultrasound time 0 min), normal heating 40 min and ultrasound heating 20 min (recorded as ultrasound time 20 min), normal heating 20 min and ultrasound heating 40 min (recorded as ultrasound time 40 min), and ultrasound heating 60 min (recorded as ultrasound time 60 min) were studied respectively. The effects of ultrasound time on t_{trans} and the quality of recovered crystals were investigated under the conditions of an ultrasound power of 360 W, a stirring rate of 200 RPM, and a solution pH of 7, and the results are shown in Fig. 5(a). The particle sizes of different products were determined, as shown in Fig. 5(b).

Compared with the normal crystallization (recorded as an ultrasound time of 0 min), the addition of ultrasound significantly shortens t_{trans} and increases the yield of ammonium sulfate, regardless of whether the ultrasound time is 20, 40, or 60 min. Ultrasound can promote heat and mass transfer effects in the solution during the crystallization process [29], resulting in an increase in ammonium sulfate yield and a decrease in t_{trans} as the ultrasound time increases from 20 to 60 min. However, the effects of ultrasound time on t_{trans} , ammonium sulfate yield and particle size distribution are not significant, as shown in Fig. 5(a) and 5(b). This is because the promoting effect of ultrasound on crystallization occurs mainly during the crystal nucleation and growth stages, rather than in the early stages of heating when a large amount of water evaporates. When the ultrasound time is 20–60 min and the total heating time is controlled to 60 min, the t_{trans} is 49–50 min; that is, it takes 49–50 min of heating to observe the formation of crystal nuclei, while the growth of crystal nuclei only takes up 10–11 min. If the ultrasound time is controlled to 40 or 60 min, a large amount of ultrasound energy will be used to evaporate the water, resulting in waste. By controlling the ultrasound time to 20 min, ultrasound can be effectively utilized for crystal nucleation formation and growth. Therefore, an ultrasound time

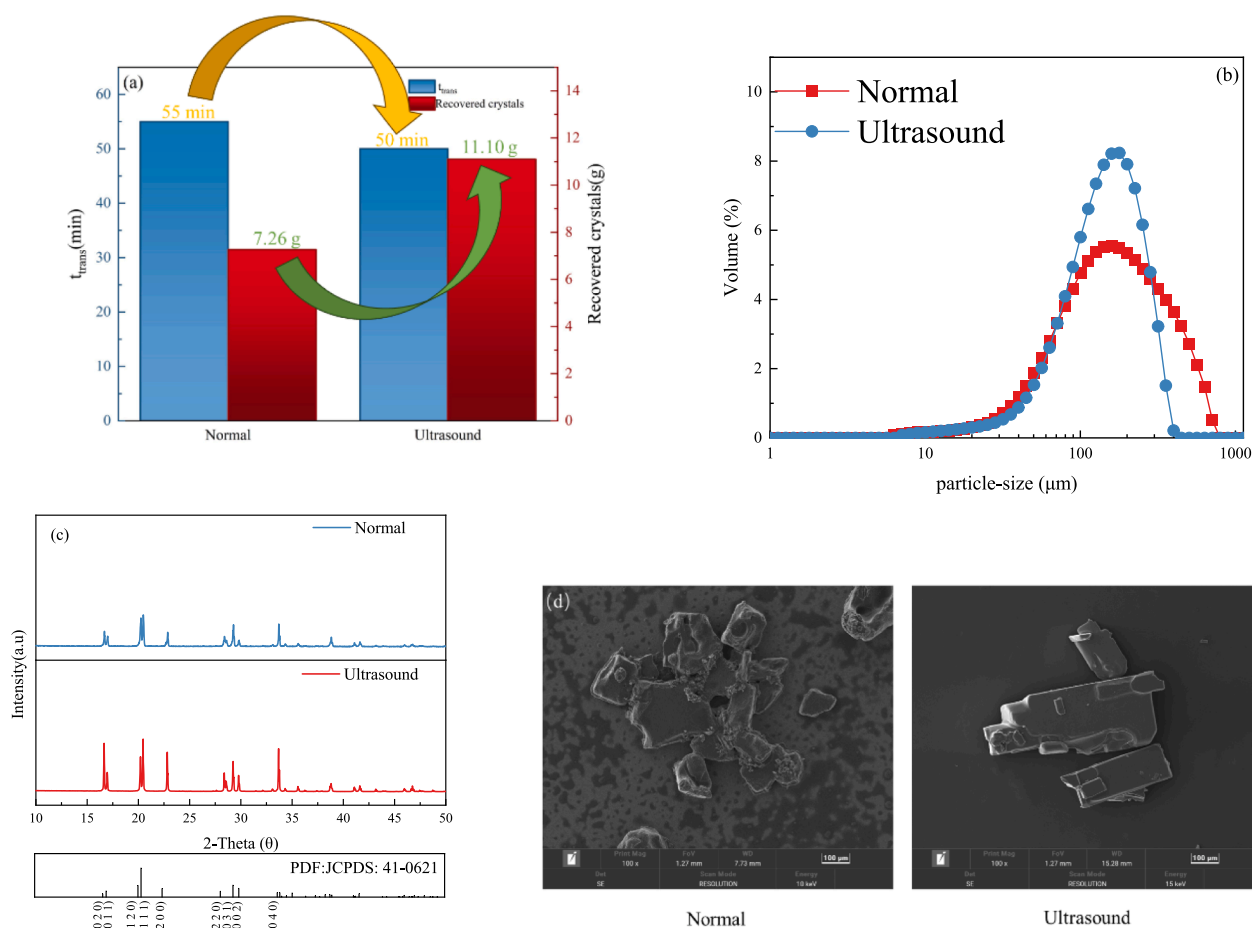


Fig. 6. The quality of recovered crystals and t_{trans} (a), crystal particle size(b), XRD patterns (c) and SEM images (d) of the ammonium sulfate products obtained by normal and ultrasound crystallizations.

of 20 min is selected as the optimal condition in this study.

3.2. The strengthening mechanism of ultrasound on ammonium sulfate crystallization

3.2.1. Comparison of normal and ultrasound crystallization products

The total crystallization time was controlled to 60 min. A normal ammonium sulfate product was obtained after normal heating for 60 min with a stirring rate of 200 RPM, and a solution pH of 7. An ultrasound ammonium sulfate product was obtained after normal heating for 40 min and then ultrasound heating for 20 min with an ultrasound power of 360 W, a stirring rate of 200 RPM, and a solution pH of 7. The t_{trans} and the quality of recovered crystals of the two products are shown in Fig. 6(a). The particle sizes, XRD patterns, and SEM images of the two ammonium sulfate products are shown in Fig. 6(b), (c), and (d), respectively.

As shown in Fig. 6(a) and (b), compared with normal crystallization, ultrasound crystallization can reduce the t_{trans} by 10 %, increase the quality of recovered crystals by 52.9 %, and obtain more uniform and smaller ammonium sulfate particles. The addition of ultrasound promotes the growth of each crystal plane of ammonium sulfate, resulting in a stronger characteristic peak intensity for each crystal face, indicating that ultrasound promotes the crystallization of ammonium sulfate than normal crystallization (Fig. 6(c)). A comparison of the SEM images in Fig. 6(d) shows that the ammonium sulfate particles obtained from normal crystallization exhibit irregular agglomeration, while the ammonium sulfate crystals obtained ultrasound crystallization have a more regular shape.

3.2.2. Strengthening mechanism of ammonium sulfate crystallization by ultrasound

The change in temperature of ammonium sulfate solution with time was tested under ultrasound heating time or normal heating time, and the results are shown in Fig. 7(a). Cavitation bubbles that formed under the action of ultrasound waves form high temperatures and high pressures in the microarea at the moment of rupture. Coupled with the strong stirring effect of ultrasound, heat transfer in solution increases [29–31], resulting in a higher solution temperature under ultrasound than under normal heating conditions. In addition, the shock wave, high temperature and high pressure caused by ultrasound cavitation effect strengthen the mass transfer of ammonium sulfate and promote the formation of ammonium sulfate crystals. During the process of crystal growth, the shock wave generated by ultrasound causes normally grown agglomerated large crystal grains to form more small crystal nuclei, thus promoting further crystallization of ammonium sulfate [27,32]. Therefore, the yield of ammonium sulfate when using ultrasound enhanced evaporation crystallization is much higher than that when using the normal method.

When the solute concentration in the solution is higher than the equilibrium concentration at the desired temperature, crystal nucleation and subsequent crystal growth occur [9]. Supersaturation, the difference between the actual concentration of a solution and its equilibrium concentration, is considered to be the driving force for crystallization [33]. When the solution is in a supersaturated state, the limiting solubility of the solute, that is, the actual concentration of the solution at that time, is called the supersolubility of the solute. The difference in the effect of crystallization between different processes can be compared by

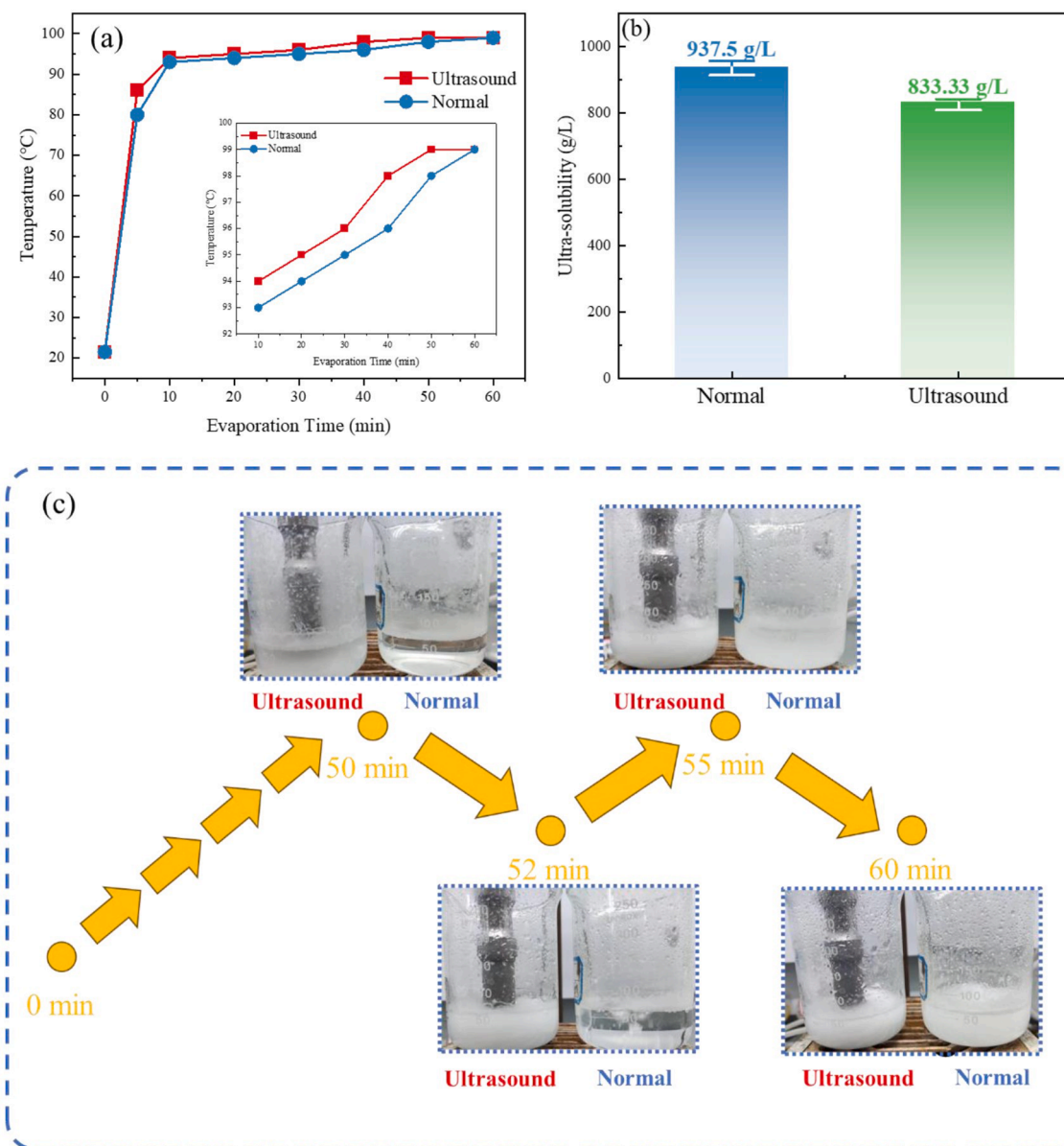


Fig. 7. Temperature-time curves (a) and the supersolubility (b) of ammonium sulfate solutions under ultrasound and normal heating. Photographs of crystallization of ammonium sulfate solution under ultrasound and normal conditions(c).

comparing the supersolubility of the solution [34,35]. In this study, the supersolubility of ammonium sulfate under ultrasound and normal crystallization at optimum reaction conditions was calculated by the volume of ammonium sulfate solution at the moment when the solid was precipitated by evaporation crystallization. The experiment was repeated 6 times in total, and the average supersolubility results are shown in Fig. 7(b). The supersolubility of ammonium sulfate decreases from 937.5 g/L for normal crystallization to 833.33 g/L for ultrasound crystallization, indicating that the introduction of ultrasound can reduce the supersolubility of ammonium sulfate solution during the evaporation crystallization process, allowing ammonium sulfate to precipitate crystals at lower concentrations than normal crystallization under ultrasound action, thereby promoting the precipitation of ammonium sulfate crystals. Similar phenomena have also been reported in other works. Sun et al.[35] investigated the supersolubility of lithium carbonate with no seed crystals, and found that the solubility of lithium carbonate decreased from 0.59 mol/L (20 °C) and 0.48 mol/L (40 °C) to 0.55 mol/L and 0.43 mol/L, respectively, after adding ultrasound. Dong et al.[36] reported that the supersolubility of p-Xylene decreased from

83 g/100 g solution to 77 – 79 g/100 g solution after ultrasound treatment at 276 K (3 °C), and the supersolubility gradually decreased with increasing ultrasound power. The reason why ultrasound reduces the supersolubility can be attributed to the cavitation effect of ultrasound. Under the action of ultrasound, many tiny cavitation bubbles are generated in the solution. When the cavitation bubbles collapse suddenly, local areas with high temperatures above 5000 K and high pressures of about 50 MPa are formed, resulting in a rapid increase in the actual concentration of solutes in these local areas and the precipitation of fine crystals. However, the actual concentration of solutes in areas other than high temperature and high pressure still remains at a low level, so the average actual concentration of ammonium sulfate in the entire solution is at a relatively low level. We observed that compared to normal crystallization, ultrasonic crystallization resulted in crystal precipitation of ammonium sulfate solution at lower supersolubility. The result is that under the same heating time, ammonium sulfate precipitates earlier during the ultrasound crystallization process than during the normal crystallization process, as shown in Fig. 7(c). In addition, in this study, the supersolubility of ammonium sulfate under both

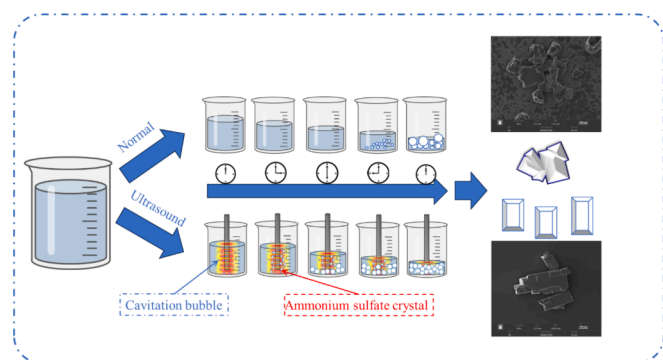


Fig. 8. Schematic diagram of the mechanism by which ultrasound affects the evaporating crystallization of ammonium sulfate.

ultrasound crystallization and normal crystallization conditions was lower than the theoretical value of pure ammonium sulfate solution at the same temperature (about 941–1030 g/L [37]). This phenomenon may be due to the presence of 20 g/L ammonium sulfate impurities in the desulfurization simulation solution, which promoted the crystallization of ammonium sulfate.

The mechanism by which ultrasound enhances the evaporating crystallization of ammonium sulfate is shown in Fig. 8. Due to the cavitation effect of ultrasound, tiny crystals precipitate early in the local area of the solution, enabling the solution to precipitate crystals under lower supersolubility conditions than in normal crystallization processes, enhancing the crystallization effect. Subsequently, when ammonium sulfate crystal nuclei are formed in solution, the mechanical action of ultrasound waves breaks the agglomerated large crystals into pieces, forming more secondary crystal nuclei and making the particles uniform. Therefore, introducing ultrasound during the evaporating crystallization of ammonium sulfate solution at atmospheric pressure can significantly shorten the crystallization time of ammonium sulfate, increase the yield of ammonium sulfate, and obtain ammonium sulfate crystals with higher crystallinity and more uniform particle sizes.

4. Conclusions

Ultrasound was introduced to enhance the evaporating crystallization of ammonium sulfate at atmospheric pressure in this work. The optimal reaction conditions were obtained after normal heating for 40 min and then ultrasound heating for 20 min with an ultrasound power of 360 W, a stirring rate of 200 RPM, and a solution pH of 7. Compared with entire normal crystallization, ultrasound crystallization can reduce the solid–liquid transformation time (t_{trans}) by 10 %, increase the quality of recovered crystals by 52.9 %, and obtain more uniform and highly crystalline ammonium sulfate products. The mechanism of ultrasound-induced ammonium sulfate crystallization is mainly by strengthening the collisions between ammonium sulfate molecules in the solution to reduce the supersolubility of the ammonium sulfate solution, so that the ammonium sulfate crystals can precipitate at a lower concentration and in a shorter time. Subsequently, the mechanical action of ultrasound waves breaks the agglomerated large crystals into pieces, forming more secondary crystal nuclei and more uniform particles, thereby improving the quality of recovered ammonium sulfate crystallization products. This work lays an experimental foundation for the introduction of ultrasound to the ammonium sulfate atmospheric evaporation crystallization process.

CRedit authorship contribution statement

Haoran Xu: Writing – original draft, Methodology, Formal analysis, Data curation. **Guang Fu:** Funding acquisition. **Duclenh Phan:** Writing – review & editing. **Liuxin Xiang:** Formal analysis. **Thiquynhxuan Le:**

Writing – review & editing, Project administration, Conceptualization. **Libo Zhang:** Supervision, Resources.

Declaration of competing interest

The authors declare that they have no known competing financial interests or personal relationships that could have appeared to influence the work reported in this paper.

Acknowledgement

Funding: This work was financially supported by the Yunnan Fundamental Research Projects [202101BE070001-023 and 202201AU070088], Yunnan Major Scientific and Technological Project (202302AG050008), and “Yunnan Revitalization Talents Support Plan” -High-end Foreign Talents Program.

References

- [1] A. Kumar, S. Dubey, Utilization of natural gypsum for the preparation of ammonium sulfate, *Chem. Pap.* 77 (5) (2023) 2707–2716, <https://doi.org/10.1007/s11696-022-02660-9>.
- [2] D.S. Powlson, C.J. Dawson, Use of ammonium sulphate as a sulphur fertilizer: Implications for ammonia volatilization, *Soil Use Manag.* 38 (1) (2022) 622–634, <https://doi.org/10.1111/sum.12733>.
- [3] H. Yang, A. Sha, Z. He, C. Wu, Y. Xu, J. Hu, Z. Xu, C. Ruan, Leaching kinetics and permeability of polyethyleneimine added ammonium sulfate on weathered crust elution-deposited rare earth ores, *J. Rare Earths* (2023), <https://doi.org/10.1016/j.jre.2023.08.022>.
- [4] H. Wang, X. Wang, Y. Wang, D. Wang, K. Hu, W. Zhong, Z. Guo, Influence of ammonium sulfate leaching agent on engineering properties of weathered crust elution-deposited rare earth ore, *Acta Geotech.* (2023), <https://doi.org/10.1007/s11440-023-01999-x>.
- [5] W. Li, T. Wang, Y. Yang, M. Fang, X. Gao, Calcium recovery from waste carbide slag via ammonium sulfate leaching system, *Journal of Cleaner Production* 377 (2022) 134308, <https://doi.org/10.1016/j.jclepro.2022.134308>.
- [6] Y. Tang, B. Zhang, H. Xie, X. Qu, P. Xing, H. Yin, Recovery and regeneration of lithium cobalt oxide from spent lithium-ion batteries through a low-temperature ammonium sulfate roasting approach, *J. Power Sources* 474 (2020) 228596, <https://doi.org/10.1016/j.jpowsour.2020.228596>.
- [7] J. Nyvlt, Effect of additives on crystallization of ammonium sulphate, *Hung. J. Ind. Chem.* 27 (2) (1999) 155–159.
- [8] X. Liu, Q. Zhong, J. Wang, X. Ji, Y. Jia, Y. Xu, L. Li, Study on ammonium sulfate crystallization in the ammonium desulphurization process in a coal-based power plant in the petrochemical industry, *Energy Sources Part A-Recovery Utilization and Environmental Effects* 33 (22) (2011) 2027–2035, <https://doi.org/10.1080/15567036.2010.499412>.
- [9] K.M. Jim, K.-J. Kim, Y.-N. Jang, Effect of supersaturation on the particle size of ammonium sulfate in semibatch evaporative crystallization, *Ind. Eng. Chem. Res.* 52 (32) (2013) 11151–11158, <https://doi.org/10.1021/ie4007968>.
- [10] L. Li, B. Huang, G. Zhang, D. Wang, M. Dai, Z. Yang, C. Wang, Optimization of ammonium sulfate crystals based on orthogonal design, *J. Cryst. Growth* 570 (2021) 126217, <https://doi.org/10.1016/j.jcrysgro.2021.126217>.
- [11] G. Zi, B. Huang, M. Dai, Z. Shi, Z. Wen, W. Li, L. Luo, L. Yang, Effects of seed crystal concentration, pH, and stirring rate on ammonium sulfate crystallization under the action of ammonium nitrate, *Phosphorus Sulfur Silicon Relat. Elem.* 198 (7) (2023) 566–574, <https://doi.org/10.1080/10426507.2023.2175828>.
- [12] G. Zi, B. Huang, M. Dai, Z. Shi, Z. Wen, W. Li, L. Luo, L. Yang, Optimization of ammonium sulfate crystallization under ammonium nitrate based on response surface method, *Cryst. Res. Technol.* 58 (3) (2023) 2200246, <https://doi.org/10.1002/crat.202200246>.
- [13] J. Peng, Z. Yang, P. Lian, Process optimization and crystallization kinetics of ammonium sulfate from wet ammonia-based desulfurization, *Environmental Progress & Sustainable Energy* (2023) 14310, <https://doi.org/10.1002/ep.14310>.
- [14] J. Park, W. Lee, J.K. Choe, Y. Choi, Non-evaporative solid phase ammonium sulfate separation from ammonia-stripped sulfuric acid solution by solvent-driven fractional crystallization, *Sep. Purif. Technol.* 318 (2023) 123869, <https://doi.org/10.1016/j.seppur.2023.123869>.
- [15] Y. Hua, Y. Bao, G. Yu, W. Zhou, H. Sun, Study on crystallization problem of ammonia desulfurization, *Guangzhou Chemical Industry* 50 (14) (2022) 186–188.
- [16] M. Ghosh, V. Venkatesan, A.K. Sikder, N. Sikder, Preparation and characterisation of ϵ -CL-20 by solvent evaporation and precipitation methods, *Def. Sci. J.* 62 (6) (2012).
- [17] A. Hu, J. Zheng, T. Qiu, Industrial experiments for the application of ultrasound on scale control in the Chinese sugar industry, *Ultrason. Sonochem.* 13 (4) (2006) 329–333, <https://doi.org/10.1016/j.ulsonch.2005.05.005>.
- [18] A.V. Mohod, P.R. Gogate, Improved crystallization of ammonium sulphate using ultrasound assisted approach with comparison with the conventional approach, *Ultrason. Sonochem.* 41 (2018) 310–318, <https://doi.org/10.1016/j.ulsonch.2017.09.047>.

- [19] R. Lakerveld, N.G. Verzijden, H. Kramer, P. Jansens, J. Grievink, Application of ultrasound for start-up of evaporative batch crystallization of ammonium sulfate in a 75-L crystallizer, *AIChE J* 57 (12) (2011) 3367–3377, <https://doi.org/10.1002/aic.12553>.
- [20] C. Mateu-Royo, J. Navarro-Esbrí, A. Mota-Babiloni, F. Molés, M. Amat-Albuixech, Experimental exergy and energy analysis of a novel high-temperature heat pump with scroll compressor for waste heat recovery, *Appl. Energy* 253 (2019) 113504, <https://doi.org/10.1016/j.apenergy.2019.113504>.
- [21] C. Liu, W. Han, X. Xue, Experimental investigation of a high-temperature heat pump for industrial steam production, *Appl. Energy* 312 (2022) 118719, <https://doi.org/10.1016/j.apenergy.2022.118719>.
- [22] S. Aswathappa, L. Dai, S.S. Jude Dhas, S.A.M.B. Dhas, E. Palaniyasan, R.S. Kumar, A.I. Almansour, Experimental evidence of acoustic shock wave-induced dynamic recrystallization: A case study on ammonium sulfate, *Cryst. Growth Des.* 24 (1) (2024) 491–498, <https://doi.org/10.1021/acs.cgd.3c01180>.
- [23] Y. Gao, Z. Meng, Crystallization of lipids and lipid emulsions treated by power ultrasound: A review, *Crit. Rev. Food Sci. Nutr.* (2022) 1–12.
- [24] R. Pathak, S.K. Bhangu, G.J. Martin, F. Separovic, M. Ashokkumar, Ultrasound-induced protein restructuring and ordered aggregation to form amyloid crystals, *Eur. Biophys. J.* 51 (4–5) (2022) 335–352.
- [25] X. Xu, Y. Zhang, Y. Yang, P. Zheng, F. Yang, Effect mechanism of fly ash on crystallization of $(\text{NH}_4)_2\text{SO}_4$ in flue gas desulfurization by ammonia process, *Chinese Journal of Environmental Engineering* 16 (08) (2022) 2621–2629, in Chinese.
- [26] Z. Yang, Y. Zuo, L. Dai, L. Zhang, Y. Yu, L. Zhou, Effect of ultrasonic-induced selenium crystallization behavior during selenium reduction, *Ultrason. Sonochem.* 95 (2023), <https://doi.org/10.1016/j.ultsonch.2023.106392>.
- [27] L.M. Belca, A. Ručigaj, D. Teslić, M. Krajnc, The use of ultrasound in the crystallization process of an active pharmaceutical ingredient, *Ultrason. Sonochem.* 58 (2019) 104642, <https://doi.org/10.1016/j.ultsonch.2019.104642>.
- [28] Y. Zheng, Y. Shen, Y. Ma, J. Wang, X. Wu, M. Yang, M. Xu, Y. Tian, Nucleation, growth, and aggregation kinetics of KCl produced by stirred crystallization, *Appl. Phys. A* 129 (9) (2023) 651, <https://doi.org/10.1007/s00339-023-06925-2>.
- [29] F. Baffigi, C. Bartoli, Influence of the ultrasounds on the heat transfer in single phase free convection and in saturated pool boiling, *Exp. Therm Fluid Sci.* 36 (2012) 12–21, <https://doi.org/10.1016/j.expthermflusci.2011.07.012>.
- [30] A.E. Bergles, P.H. Newell, The influence of ultrasonic vibrations on heat transfer to water flowing in annuli, *Int. J. Heat Mass Transf.* 8 (10) (1965) 1273–1280, [https://doi.org/10.1016/0017-9310\(65\)90055-4](https://doi.org/10.1016/0017-9310(65)90055-4).
- [31] G. Zeng, H. Li, S. Luo, X. Wang, J. Chen, Effects of ultrasonic radiation on induction period and nucleation kinetics of sodium sulfate, *Korean J. Chem. Eng.* 31 (2014) 807–811.
- [32] S.V. Dalvi, M.D. Yadav, Effect of ultrasound and stabilizers on nucleation kinetics of curcumin during liquid antisolvent precipitation, *Ultrason. Sonochem.* 24 (2015) 114–122, <https://doi.org/10.1016/j.ultsonch.2014.11.016>.
- [33] J. Jordens, B. Gielen, C. Xiouras, M.N. Hussain, G.D. Stefanidis, L.C.J. Thomassen, L. Braeken, T. Van Gerven, Sonocrystallisation: Observations, theories and guidelines, *Chemical Engineering and Processing-Process Intensification* 139 (2019) 130–154, <https://doi.org/10.1016/j.cep.2019.03.017>.
- [34] H.N. Kim, K.S. Suslick, The effects of ultrasound on crystals: Sonocrystallization and sonofragmentation, *Crystals* 8 (7) (2018), <https://doi.org/10.3390/cryst8070280>.
- [35] Y. Sun, X. Song, J. Wang, Y. Luo, J. Yu, Unseeded supersolubility of lithium carbonate: Experimental measurement and simulation with mathematical models, *J. Cryst. Growth* 311 (23) (2009) 4714–4719, <https://doi.org/10.1016/j.jcrysgro.2009.09.013>.
- [36] J. Dong, J. Wang, S. Wang, J. Wen, Experimental Investigation of p-Xylene crystallization characteristics and ultrasound enhancement mechanism, *Ind. Eng. Chem. Res.* 61 (51) (2022) 18894–18905, <https://doi.org/10.1021/acs.iecr.2c03204>.
- [37] D.R. Lide, *CRC handbook of chemistry and physics*, CRC Press, 2004.